

## Ballistic chain-chain aggregation in $d=1-3$

This article has been downloaded from IOPscience. Please scroll down to see the full text article.

1990 J. Phys. A: Math. Gen. 23 1421

(<http://iopscience.iop.org/0305-4470/23/8/015>)

View [the table of contents for this issue](#), or go to the [journal homepage](#) for more

Download details:

IP Address: 129.252.86.83

The article was downloaded on 01/06/2010 at 10:05

Please note that [terms and conditions apply](#).

## Ballistic chain–chain aggregation in $d = 1-3$

Jean-Marc Debierre and Loïc Turban

Laboratoire de Physique du Solide†, Université de Nancy I, BP 239, 54506 Vandœuvre-lès-Nancy, France

Received 27 September 1989, in final form 29 December 1989

**Abstract.** The on-lattice ballistic chain–chain aggregation model is studied by Monte Carlo simulations in one, two and three dimensions. The chains move along the lattice directions, with a velocity proportional to  $k^\gamma$ , for a  $k$ -mer. The fractal dimension of the large polymers and the mass distribution are computed for different values of the mobility exponent  $\gamma$ . In two and three dimensions, a long preasymptotic behaviour is observed, and in all dimensions the asymptotic behaviour is in agreement with the Smoluchowski theory.

### 1. Introduction

Numerous experimental and theoretical works have been devoted recently to the formation of large aggregates from small particles (Friedlander 1977, Herrmann 1986, Jullien and Botet 1987, Meakin 1988). A case of particular interest is Brownian aggregation: the aggregates diffuse randomly and stick irreversibly when their reactive parts come into contact. From a set of particles, this process generates ramified clusters if sticking occurs at each contact (Meakin 1983, Kolb *et al* 1983), and generates topologically linear chains if only the two end tips are reactive (Debierre and Turban 1987a). In both cases, the large aggregates have a fractal structure and the kinetics of reaction (Ziff *et al* 1985, Debierre 1989) is well described by the mean-field Smoluchowski theory (Smoluchowski 1916). Ballistic aggregation was first introduced for particle–cluster aggregation (Vold 1963). In the case of cluster–cluster ballistic aggregation, the aggregates follow straight trajectories at constant speed and stick in accordance with the same rules as above when they collide. It has been shown that the fractal dimension of ramified clusters is higher in this case (Ball and Jullien 1984), but very little is known about the kinetics of reaction.

In this paper, we present the results of computer simulations on  $d$ -dimensional lattices ( $d = 1, 2, 3$ ) for the ballistic chain–chain aggregation model. In  $d = 1$ , the chain–chain and cluster–cluster models are equivalent. The chains move along the lattice directions, with a velocity  $v(k) \sim k^\gamma$  for a chain of mass  $k$ , and we investigate the influence of the mobility exponent  $\gamma$  on the kinetics of aggregation. A similar study for the diffusion-limited version of chain–chain aggregation has already been published (Debierre and Turban 1988, Debierre *et al* 1989, hereafter referred to as I). As the two models exhibit a relatively similar behaviour, we only emphasise here the specific features of the ballistic case and refer the reader to I for more general information.

† Unité de Recherche Associée au CNRS no DO 155.

In section 2, we give a detailed description of the algorithm used for the simulations. The theoretical approach based on the dynamic scaling hypothesis and the Smoluchowski theory is reviewed in section 3. Finally, the numerical results are presented and discussed in section 4.

## 2. Computer simulations

The simulations in  $d = 1, 2$  and  $3$  are performed on  $10^5$  linear,  $400 \times 400$  triangular and  $100 \times 100 \times 100$  cubic lattices with periodic boundary conditions. At time  $t = 0$ , monomers are randomly distributed on non-adjacent lattice sites, ready to start with unit velocities, in randomly selected directions. The initial monomer concentration is respectively 10%, 2.5% and 1.5% in  $d = 1, 2$  and  $3$ . At time  $t$ , reactions have occurred and the sample contains monomers, dimers, trimers and so on. All the  $N(k, t)$  chains of mass  $k$  ( $k$ -mers) perform a uniform linear motion with an average velocity

$$v(k) \sim k^\gamma. \quad (1)$$

As for the Brownian case (I), we have varied the exponent  $\gamma$  to observe a possible change of kinetics at some value  $\gamma_c$ , and to determine the sticking exponent  $\varphi$ , for a reaction between two chains. The case  $\gamma = -\frac{1}{2}$  is of particular interest, each chain then having a velocity which corresponds to the average value for a Maxwell-Boltzmann distribution. Let us remark that there is no point in using a distribution of velocities, since momentum cannot be conserved on a lattice.

To prevent them from overlapping, the chains are moved one at a time and, at each Monte Carlo step, a  $k$ -mer is chosen randomly with probability

$$p(k, t) = k^\gamma / p_{\max} \quad (2)$$

where

$$p_{\max} = \sum_k N(k, t) k^\gamma \quad (3)$$

is a normalisation coefficient. To directly select a chain with the desired probability, the following procedure is used in our simulations. The ensemble of the chains in the sample is represented by an equivalent ensemble of adjacent segments. A segment of length  $k^\gamma$  is associated with a  $k$ -mer, so that the total length of the segments is  $p_{\max}$ . Thus, a random number evenly distributed in the interval  $[0, p_{\max}]$  has a probability  $p(k, t)$  of lying in the segment associated with a given chain of mass  $k$ .

At each Monte Carlo step, the following operations are repeated.

(i) Generate a random number in the interval  $[0, p_{\max}]$  and select the chain associated with this number.

(ii) Increment the physical time by  $\delta t$ . As a  $k$ -mer is selected with a probability  $p(k, t)$  and its jump frequency is proportional to  $k^\gamma$  (equation (1)), we have

$$\delta t = p(k, t) / k^\gamma = 1 / p_{\max}. \quad (4)$$

(iii) Translate the selected chain by one lattice unit in its direction of motion. In case some lattice sites become doubly occupied, the chain is not moved and the procedure starts from (i) again.

(iv) Examine the nearest-neighbour sites of the two chain tips successively. If the tip of *another* chain is found, make the two chains join. This last condition ensures that no closed loop is formed during a reaction.

This procedure is repeated until the final time has been reached. As it is not possible to conserve momentum on the lattice, a new direction of motion is randomly chosen for the chains involved in a reaction or a collision. Thus, after a collision, the chains may move away from each other. We have performed fifty simulations for several values of  $\gamma$  in the intervals  $[-2, 0.5]$  in  $d = 1$  and  $d = 3$ , and  $[-3, 1]$  in  $d = 2$ .

### 3. Dynamic scaling and Smoluchowski theory

To characterise the dynamical behaviour of our model, we have computed the mass distribution  $n(k, t)$ , i.e. the concentrations of  $k$ -mers at different times. We expect  $n(k, t)$  to be a solution of the Smoluchowski rate equation (Smoluchowski 1916)

$$\frac{\partial n(k, t)}{\partial t} = \frac{1}{2} \sum_{i+j=k} K(i, j)n(i, t)n(j, t) - n(k, t) \sum_{i=1}^{\infty} K(k, i)n(i, t). \quad (5)$$

This mean-field equation is valid at and above an upper critical dimension  $d_c$ . It has been conjectured (Toussaint and Wilczek 1983, Kang and Redner 1984) that in the Brownian case,  $d_c = 2$  for  $A + A \rightarrow A$  and  $A + A \rightarrow O$  reactions and an extension of this argument for the ballistic  $A + A \rightarrow O$  reactions gives  $d_c = 1$ . However, it has been shown very recently (van Dongen 1989) that, for Brownian aggregation,  $d_c = 2$  is not always true. In this case,  $d_c$  depends on the details of the model and, for  $d < d_c$ , the Smoluchowski approach breaks down at a characteristic time  $t_D$  after which the kinetics becomes that of diffusion-limited aggregation, independent of the initial model. As the ballistic case has not been discussed in this work, the mean-field approach will still be used here to analyse our data.

For simple aggregation models, the reaction kernel  $K(i, j)$  is usually a homogeneous function, i.e.

$$K(ai, aj) = a^\lambda K(i, j) \quad (6a)$$

$$K(i, j) \sim i^\mu j^\nu \quad i \ll j \quad (i \gg 1). \quad (6b)$$

In this case, equation (5) admits solutions of the form

$$n(k, t) = t^{-2z} g(x) \quad (7)$$

where  $x = k/\bar{k}$  is the scaling variable. At large times, the mean chain mass  $\bar{k}$  varies as

$$\bar{k} \sim t^{1/(1-\lambda)} \sim t^z \quad (8)$$

and the dynamic exponent  $z$  is positive for non-gelling systems ( $\lambda \leq 1$ ). For  $x \gg 1$ , the scaling function  $g(x)$  decreases exponentially, and for  $x \ll 1$  three classes of kinetics are possible, according to the sign of  $\mu$  (van Dongen and Ernst 1985):

$$\text{class I} \quad \mu > 0 \quad g(x) = Bx^{-\tau} \quad \tau = 1 + \lambda \quad (9a)$$

$$\text{class II} \quad \mu = 0 \quad g(x) = Bx^{-\tau} \quad \tau < 1 + \lambda \quad (9b)$$

$$\text{class III} \quad \mu < 0 \quad g(x) \sim \exp(-bx^\mu) \quad b > 0. \quad (9c)$$

It follows that the large-time behaviour of the total number of chains  $N(t)$  is given by

$$N(t) \sim t^{-z} \quad \text{class III or } \tau \leq 1 \quad (10a)$$

$$N(t) \sim t^{-\mu} \quad \tau > 1 \quad (10b)$$

with

$$w = (2 - \tau)z. \quad (11)$$

In analogy with Brownian chain-chain aggregation (I), one writes the reaction kernel for the ballistic case as

$$K(i, j) \sim (i^{2\gamma} + j^{2\gamma})^{1/2} (i^{1/D} + j^{1/D})^{d-1} h(i, j) \quad (12)$$

where  $h(i, j)$  is the sticking probability between an  $i$ -mer and a  $j$ -mer. The first factor is the root mean square relative velocity which replaces here the relative diffusion coefficient of the Brownian case (I). The second factor is an effective cross-section for collision which depends on the chain fractal dimension  $D$ : two chains of radius  $R_i \sim i^{1/D}$  and  $R_j \sim j^{1/D}$  occupy together a sphere of influence of volume  $V = (R_i + R_j)^d$  with a cross section  $V^{(d-1)/d}$ . If we assume  $h(i, j)$  to be a homogeneous function of degree  $-\varphi$ , then the overall homogeneity degree of the kernel is

$$\lambda = \gamma + (d - 1)/D - \varphi \quad (13)$$

and, as a consequence of equation (8), the dynamic exponent  $z$  is related to the mobility exponent by

$$z^{-1} = [1 - (d - 1)/D + \varphi - \gamma]. \quad (14)$$

#### 4. Discussion of the results

The fractal dimension  $D(d)$  of the chains has been extracted from the radius of gyration data. In  $d = 1$ , the chains are obviously linear and  $D(1) = 1$ . In  $d = 2$  and  $3$ , the average values of the fractal dimension are respectively  $D(2) = 1.38 \pm 0.04$  and  $D(3) = 1.68 \pm 0.05$ , the error bars resulting from small deviations of the estimates obtained for the different  $\gamma$ . However, the variations of  $D$  with  $\gamma$  do not appear to be systematic and we conclude that  $D$  is independent of  $\gamma$  for the values considered here. The average  $D$  values are slightly higher than those of the self-avoiding walk model ( $\frac{4}{3}$  and  $\frac{5}{3}$  respectively) and very close to those obtained in the case of Brownian (I) or free-reptation-limited (Debierre and Turban 1987b) aggregation. Thus, unlike for ramified clusters (Ball and Jullien 1984, Jullien 1984, Jullien and Kolb 1984, Meakin and Family 1987), the static properties of large chains appear to be unaffected by the nature of the motion they undergo.

The asymptotic behaviour of the total number of chains  $N$  and the mean chain mass  $\bar{k}$  predicted by equations (10) and (8) is effectively observed in our simulations. At large time,  $\ln N$  and  $\ln \bar{k}$  become linear functions of  $\ln t$  and linear fits of the curves in figures 1 and 2 give the estimates of the dynamic exponent  $z$  listed in table 1. In  $d = 1$ , for  $0 \leq \gamma \leq 0.25$  we observe a behaviour of type (10b), with  $w$  given in table 1, so that we expect  $\tau > 1$  in this case. This may be checked by the small- $x$  behaviour of the scaling function  $g(x)$  which is plotted in figure 3, for a representative set of  $\gamma$  values, in  $d = 1-3$ . In all dimensions,  $g(x)$  is a monotonically decreasing function for  $\gamma \geq 0$ , thus the kinetics is necessarily in class I or II and  $\tau$  is given by the slope of the left-hand part of the curves in figure 3. These estimates are listed in table 1: as expected, in  $d = 1$  we have  $\tau > 1$  for  $\gamma \leq 0.25$  and the scaling law (11) is verified. We also note in table 1 that, for  $\gamma \geq 0$ , the condition  $\tau < 1 + \lambda$  (9b) for class II kinetics which, using (8), becomes

$$\tau + z^{-1} < 2 \quad (15)$$

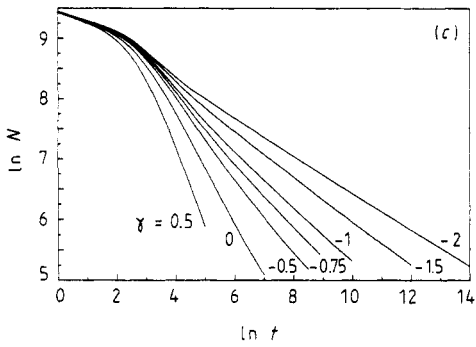
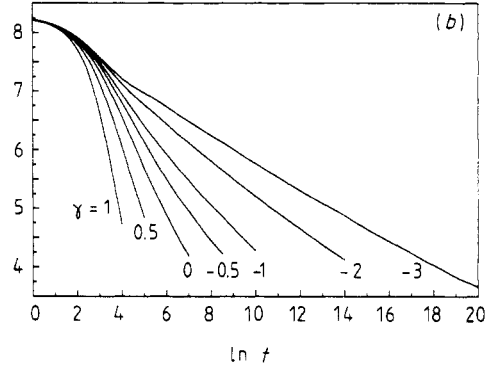
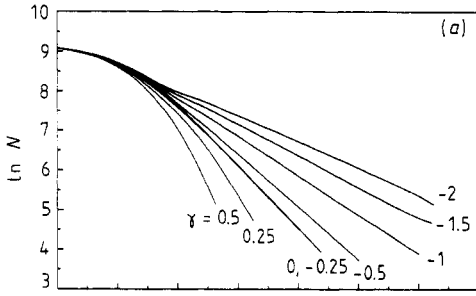


**Figure 1.** Log-log plot of the total number of chains  $N$  as a function of the time  $t$ , in (a) one, (b) two and (c) three dimensions.

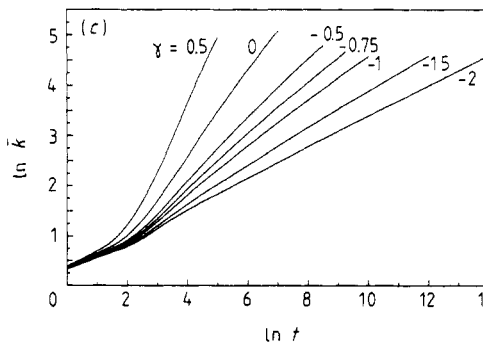
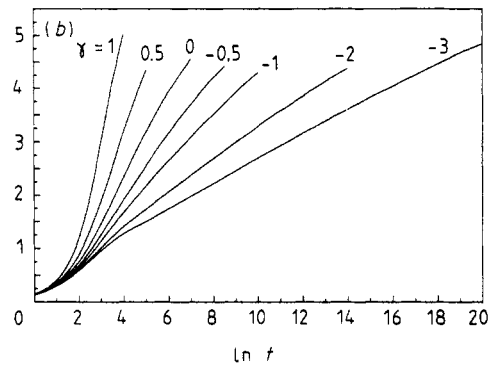
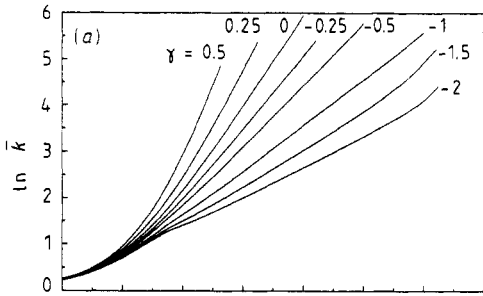


**Figure 2.** Log-log plot of the mean chain mass  $\bar{k}$  as a function of the time  $t$ , in (a) one, (b) two and (c) three dimensions.

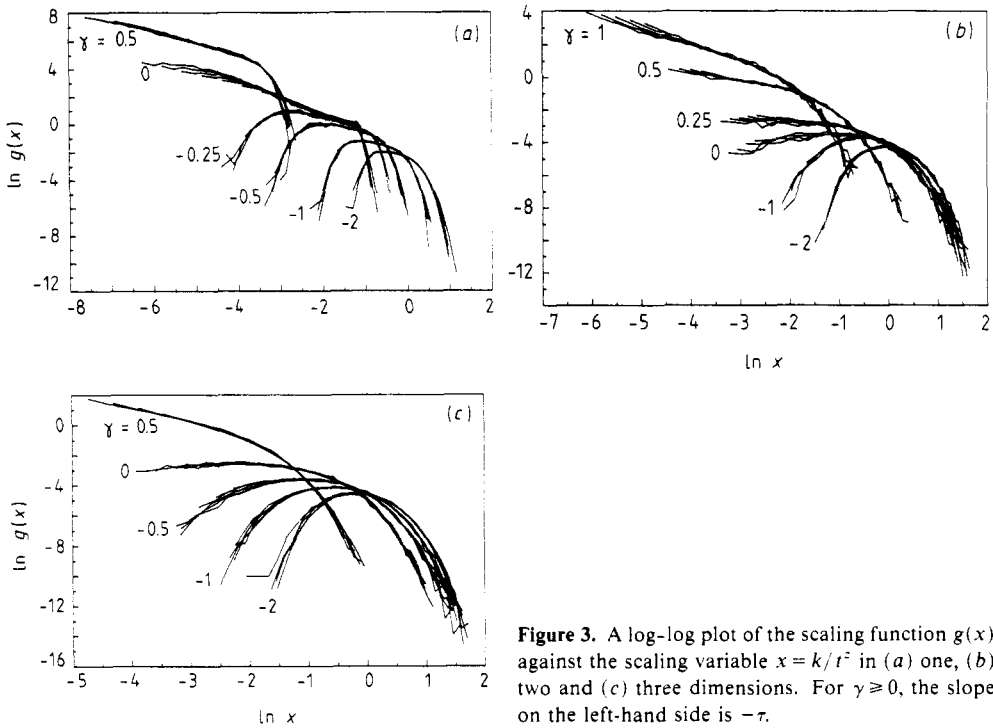


**Figure 3.** A log-log plot of the scaling function  $g(x)$  against the scaling variable  $x = k/t^2$  in (a) one, (b) two and (c) three dimensions. For  $\gamma \geq 0$ , the slope on the left-hand side is  $-\tau$ .

appears to be satisfied in all dimensions. Then, from equations (8) and (9b), we expect a class II kinetics with  $\mu = 0$ .

When  $\gamma < 0$ , the scaling function  $g(x)$  is bell shaped (figure 3) and we may have either a class I or II kinetics with  $\tau < 0$  or a class III kinetics. When  $i \ll j$  ( $i \gg 1$ ), the asymptotic form of the sticking probability  $h(i, j) \sim i^\alpha j^\beta$  inserted into equation (6b) gives  $\mu = \alpha + \gamma$ . If we assume that, as for Brownian chain-chain aggregation (Debierre 1989),  $h(i, j)$  is a non-increasing function of  $i$  and  $j$ , then  $\alpha < 0$  and as a consequence  $\mu < 0$ , indicating a class III kinetics.

In conclusion, in  $d = 1-3$  we conjecture a change from class II kinetics for  $\gamma \geq 0$  to class III kinetics for  $\gamma < 0$ . This conjecture is in agreement with the Smoluchowski theory in one dimension: as in  $d = 1$  each collision is effective, the sticking probability is equal to 1 and equations (12) and (6b) give  $\mu = 0$  for  $\gamma \geq 0$  and  $\mu < 0$  for  $\gamma < 0$ . One possible reason why condition (15) is not always verified numerically in  $d = 1$  (see table 1) is the existence of logarithmic corrections to the asymptotic behaviour when  $d = d_c$ . In two and three dimensions (figures 3(b) and 3(c)), the mass distribution for  $\gamma = 0$  is uniform ( $\tau = 0$ ) and the change from polydispersity to monodispersity at  $\gamma = 0$  is smooth. On the contrary, this change is abrupt in one dimension (figure 3(a)) since the distribution for  $\gamma = 0$  is not uniform ( $\tau = 1.2$ ).

Finally we consider the variations of the dynamic exponent  $z$  with  $\gamma$ . In one dimension,  $\varphi$  is zero because each collision is effective and equation (14) reduces to

$$z^{-1} = 1 - \gamma \tag{16}$$

which is remarkably well verified by our numerical  $z$  values (figure 4(a)). In higher dimensions, it is more difficult to accurately estimate the dynamic exponent  $z$  because

**Table 1.** The dynamic exponents  $z$  and  $\tau$ , for  $d = 1-3$ . The exponent  $w$  is also indicated in brackets when  $\tau \geq 1$ . From the Smoluchowski theory, a class II kinetics is predicted when  $\tau + z^{-1} < 2$  and a class III kinetics for  $\gamma < 0$ .

$d$	$\gamma$	$z$	$\tau (w)$	$\tau + z^{-1}$	Class
1	-2.0	0.33	—		III
	-1.5	0.39	—		
	-1.0	0.49	—		
	-0.5	0.67	—		
	-0.25	0.79	—		
	-0.1	0.90	—		
	0	0.96	1.2 (0.79)	2.24	II
	0.1	1.06	1.1 (0.98)	2.04	
	0.25	1.23	1.0 (1.21)	1.81	
	0.5	1.63	0.85	1.46	
2	-3.0	0.22	—		III
	-2.5	0.25	—		
	-2.0	0.28	—		
	-1.5	0.34	—		
	-1.0	0.41	—		
	-0.5	0.52	—		
	0	0.60	0	1.67	II
	0.25	0.83	0.16	1.36	
	0.5	1.1	0.54	1.45	
	0.75	1.6	0.83	1.46	
1.0	1.8	0.94	1.50		
3	-2.0	0.30	—		III
	-1.5	0.35	—		
	-1.0	0.44	—		
	-0.75	0.49	—		
	-0.5	0.57	—		
	0	0.79	0	1.27	II
	0.5	1.39	0.76	1.48	

at short times a long preasymptotic regime is observed for the first moments of the distribution (figure 5), whereas at long times the real asymptotic regime may be perturbed by a saturation effect due to the finite size of the underlying lattice. The reason is that at large times only a few chains are left in the sample and, if the majority of them move in the same direction, the reaction is drastically slowed down. This explains why we have chosen the triangular lattice for the simulations in  $d = 2$ , this saturation effect being less sensitive for a high coordination number. The variations of  $z^{-1}$  as a function of  $\gamma$  in  $d = 2$  and  $d = 3$  are displayed in figures 4(b) and 4(c) respectively. We have also reported the data corresponding to the preasymptotic regime: these points appear to be aligned along directions of slopes  $-0.7$  ( $d = 2$ ) and  $-0.8$  ( $d = 3$ ), but we have no justification for these values. On the other hand, the data for  $z^{-1}$  in the asymptotic regime vary linearly with  $\gamma$  (figures 4(b) and 4(c)) with slopes  $-1.00$  ( $d = 2$ ) and  $-1.05$  ( $d = 3$ ), in agreement with the value  $-1$  predicted by equation (14). From figures 4(b) and 4(c) we also extract the following estimates of the sticking exponent:

$$\varphi(2) = 1.28 \pm 0.08 \quad \varphi(3) = 1.43 \pm 0.05. \quad (17)$$



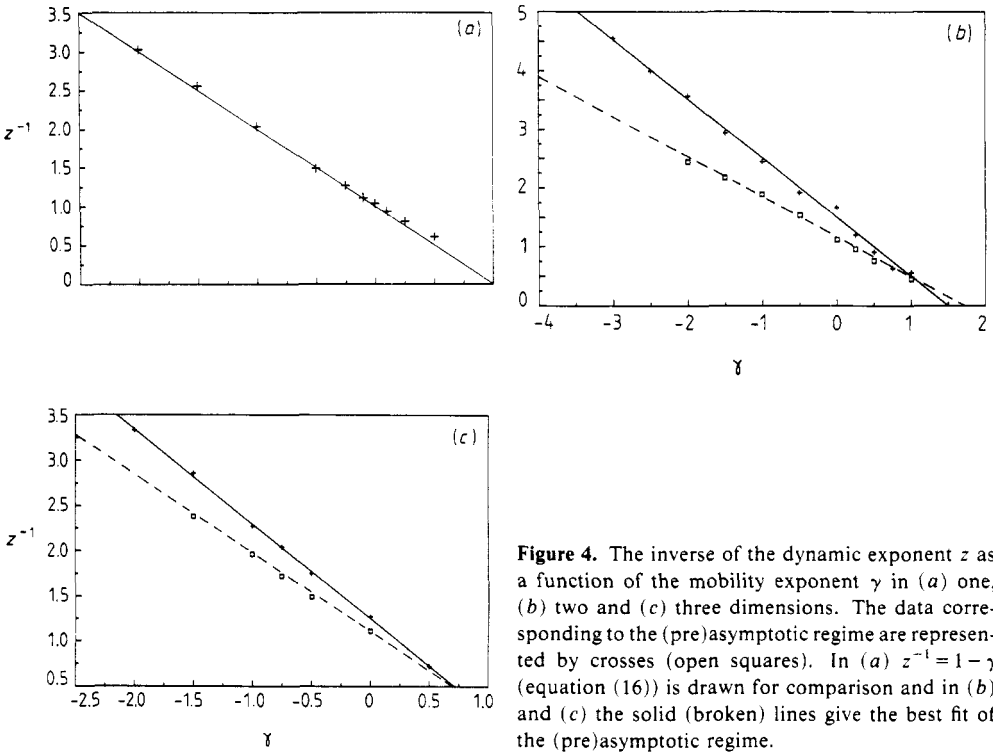


**Figure 4.** The inverse of the dynamic exponent  $z$  as a function of the mobility exponent  $\gamma$  in (a) one, (b) two and (c) three dimensions. The data corresponding to the (pre)asymptotic regime are represented by crosses (open squares). In (a)  $z^{-1} = 1 - \gamma$  (equation (16)) is drawn for comparison and in (b) and (c) the solid (broken) lines give the best fit of the (pre)asymptotic regime.

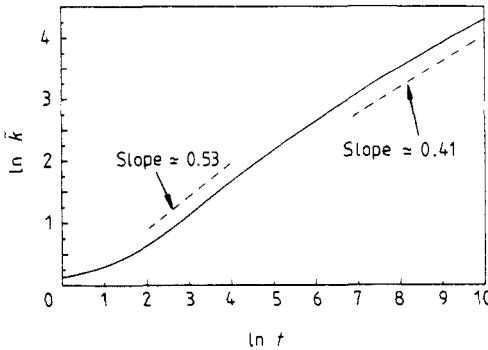


**Figure 5.**  $\ln \bar{k}$  plotted against  $\ln t$ , for  $\gamma = -1$  in two dimensions. At short times, a preasymptotic regime with  $\bar{k} \sim t^{0.53}$  is observed and the asymptotic behaviour  $\bar{k} \sim t^{0.41}$  is only reached at very long times.

The Sutherland ghost model (Ball and Witten 1984) was introduced to calculate the dimension of space  $d_t$  above which ramified clusters become mutually transparent, as well as their fractal dimension  $D_g$ . Extending this idea to the case of chains, one finds  $D_g = 2$  and  $d_t = 2D_g + d_w = 5$  (respectively, 6) for ballistic (respectively, Brownian) chain-chain aggregation. When  $d < d_t$ , the transparency assumption can be used to obtain a lower limit for the sticking exponent  $\varphi$ . We consider two transparent chains of mass  $k$  and radius  $R \sim k^{1/D}$ , in the reference frame where one of them is at rest.

The moving chain has to perform  $N_s \sim R$  steps to go through the target chain and, at each step, a reactive tip is encountered with a probability proportional to  $1/R^d$ . The sticking probability is then

$$p(k) \sim N_s/R^d \sim R^{1-d} \sim k^{(1-d)/D} \quad (18)$$

and we find the sticking exponent

$$\varphi_t(d) = (d-1)/D \quad (19)$$

for transparent chains. In the actual simulations, the chains bounce (or stick) when they meet and the transparency assumption is not correct, but it becomes more and more realistic as  $d$  is increased, since the chains can interpenetrate more and more freely. Using the  $D$  values given above, we obtain  $\varphi_t(2) = 0.72 \pm 0.02$  and  $\varphi_t(3) = 1.19 \pm 0.04$ , to be compared to the simulation results (equation (17)).

The agreement of our simulation data with the mean-field theory predictions seems to justify *a posteriori* the assumption that  $d_c = 1$  for ballistic chain-chain aggregation. A more physical approach to this phenomenon would need off-lattice simulations, with a velocity distribution for each species ( $k$ -mer). Moreover, since the reactions between the chains have to be described in terms of inelastic collisions, it would also be necessary to take into account the deformation of the chains. Performing simulations that meet all these requirements is presently a hopeless task.

### Acknowledgment

We thank the CIRCE in Orsay for providing time on the VP200 supercomputer.

### References

- Ball R and Jullien R 1984 *J. Physique Lett.* **45** L1031  
 Ball R and Witten T 1984 *J. Stat. Phys.* **36** 873  
 Debierre J-M 1989 *Phys. Rev. A* **40** 4804  
 Debierre J-M and Turban L 1987a *J. Phys. A: Math. Gen.* **20** L259  
 — 1987b *J. Phys. A: Math. Gen.* **20** 4457  
 — 1988 *J. Phys. A: Math. Gen.* **21** 1029  
 Debierre J-M, Turban L, Penson K A and Busch U 1989 *Phys. Rev. A* **39** 470  
 Friedlander S K 1977 *Smoke, Dust and Haze: Fundamentals of Aerosol Behavior* (New York: Wiley)  
 Herrmann H J 1986 *Phys. Rep.* **136** 153  
 Jullien R 1984 *J. Phys. A: Math. Gen.* L771  
 Jullien R and Botet R 1987 *Aggregation and Fractal Aggregates* (Singapore: World Scientific)  
 Jullien R and Kolb M 1984 *J. Phys. A: Math. Gen.* **17** L639  
 Kang K and Redner S 1984 *Phys. Rev. A* **30** 2833  
 Kolb M, Botet R and Jullien R 1983 *Phys. Rev. Lett.* **51** 1123  
 Meakin P 1983 *Phys. Rev. Lett.* **51** 1119  
 — 1988 *Phase Transitions and Critical Phenomena* vol 12, ed C Domb and J L Lebowitz (New York: Academic) p 322  
 Meakin P and Family F 1987 *Phys. Rev. A* **36** 5498  
 Smoluchowski M 1916 *Z. Phys.* **17** 585  
 Toussaint D and Wilczek F 1983 *J. Chem. Phys.* **78** 2642  
 van Dongen P G J 1989 *Phys. Rev. Lett.* **63** 1281  
 van Dongen P G J and Ernst M H 1985 *Phys. Rev. Lett.* **54** 1396  
 Vold M 1963 *J. Colloid Sci.* **18** 684  
 Ziff, R M, McGrady E M and Meakin P 1985 *J. Chem. Phys.* **82** 5269